



CORROSION PERFORMANCE OF PLASMA NITRIDED AUSTENITIC STAINLESS STEEL IN PHOSPHATE SOLUTIONS AT pH = 6.0

Daniel MARECI,^{a*} Sorin Iacob STRUGARU,^b Corneliu MUNTEANU,^b Radu TĂRNĂUCEANU^b
and Daniel SUTIMAN^a

^a “Gheorghe Asachi” Technical University of Iași, Faculty of Chemical Engineering and Environmental Protection,
71 D. Mangeron Blvd., Iași 700050, Roumania

^b “Gheorghe Asachi” Technical University of Iași, Faculty of Mechanical Engineering, 61-63 D. Mangeron Blvd., Iași 700050, Roumania

Received September 23, 2010

Austenitic stainless steel has good corrosion resistance, but its low hardness limits use whenever surface hardness is required. Plasma nitriding is a well established technique for steel hardening that can also be applied to this kind of steels with the aim of enhancing its hardness. Austenitic stainless steel sample was plasma nitrided at a temperature of 530°C for 14 hours. Electrochemical corrosion studies were carried out with disk electrodes of nitrided austenitic stainless steel in phosphate solution at pH 6.0, using cyclic voltametry and electrochemical impedance spectroscopy (EIS) technique, comparing the results with those for untreated austenitic stainless steel. Very low corrosion current densities and passive current densities were obtained from the polarization curves, for untreated and nitrided austenitic stainless steel samples. The EIS technique was applied to study the nature of the passive film formed on untreated and nitrided austenitic stainless steel samples in phosphate solution, at open circuit potential. The results confirm that the corrosion resistance of the studied nitrided austenitic stainless steel in phosphate solution at pH 6.0 are better or similar to those of untreated austenitic stainless steel.

INTRODUCTION

Austenitic stainless steels have good corrosion resistance, but their low hardness and low wear resistance limit their use whenever surface hardness is required. Nitriding is an efficient way available to improve the mechanical and tribological properties of the material surfaces.¹ Nitriding also affects the corrosion property of stainless steel due to the diffusion of nitrogen into the steel surface. This has been well demonstrated in nitriding of austenitic stainless steel.^{2,3} Using plasma-nitriding temperatures as low as 623 K does not promote degradation in the corrosion resistance of stainless steel.⁴⁻¹¹ Gontijo *et al.*¹² carried out a series of experiments with AISI 304 L steel that was plasma-nitrided at temperature 623 to 773 K and found that the corrosion resistance degrades when the nitriding process is carried out at high temperature (723 and 773 K), due mainly

formation of CrN. Li and Bell¹³ studied the corrosion properties of plasma nitrided AISI 410 martensitic stainless steel in 3.5% NaCl and 1% HCl aqueous solutions. The electrochemical studies reveal that the nitrided samples, at temperature 420 to 500°C, showed lower corrosion rate than untreated one.¹⁴⁻¹⁶

In the present work, one austenitic stainless steel has been plasma nitrided at 530°C following the methodologies generally used in this technique. The aim was to investigate the electrochemical behaviour of these samples in a mildly corrosive environment (dehydrogeno-phosphate solution, pH = 6) using open circuit potential (E_{OC}), cyclic voltametry and electrochemical impedance spectroscopy (EIS). Results were compared with those obtained for untreated austenitic stainless steel. The electrolyte was selected in order to represent a possible borderline corrosion condition for nitrided sample, making easier the identification of any property modification in the nitrided

* Corresponding author: danmareci@yahoo.com

austenitic stainless steel with respect to the untreated austenitic stainless steel.

RESULTS AND DISCUSSION

Fig. 1 displays optical microscopy (OM) cross-sectional views of plasma nitrided austenitic stainless steel at 530°C. The OM micrographs of the nitrided sample display the austenitic matrix and, on both parts of it, a nitrided thin layer.

The open circuit potential (E_{OC}) is used as a criterion for the corrosion behaviour. Generally, materials with large negative potential values are

more reactive whilst those with large positive values are far less reactive.¹⁷

The potential-time behaviour of both untreated and nitrided austenitic stainless steels samples is shown in Fig. 2. From Fig. 2 both untreated and nitrided austenitic stainless steels samples have a tendency to form a passive film by the shift of open circuit potential (E_{OC}) to more positive (noble) direction with respect to time. An abrupt E_{OC} displacement towards positive potentials was noticed in Fig. 2 during a period of 30 minutes.



Fig. 1 – OM cross-sectional views of the plasma nitrided austenitic stainless steel.

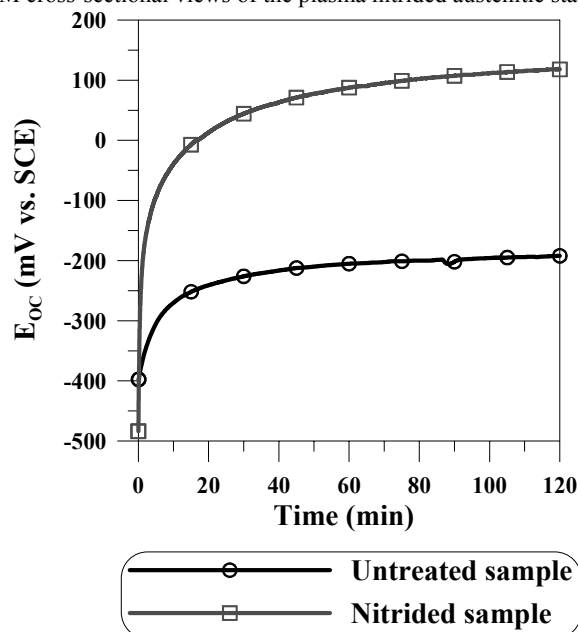


Fig. 2 – Variation of open circuit potential (E_{OC}) with time for both untreated and nitrided austenitic stainless steels samples maintained 2 hours in NaH_2PO_4 0.1 mol/L, pH 6.0.

This initial increase seems to be related to the formation and thickening of the oxide film on the metallic surface. Afterwards, the E_{OC} increases slowly suggesting the growth of the oxide film. The protecting of the oxide film increased the corrosion resistance. Stable potentials in open circuit measurements is obtained after 30 minutes exposure in NaH_2PO_4 0.1 mol/L, pH 6.0, which means the oxide film became stable. The results show that nitrided austenitic stainless steel exhibits a significantly higher open circuit potential (~ 300 mV) compared to that of the untreated alloy. The increase in E_{OC} can be attributed to passivation promoted by the presence of N. Similar observations on N enhances passivation have been previously reported and have been related to inhibition by the N at the surface.^{18,19}

Fig. 3 shows the linear polarization curves of both untreated and plasma nitrided austenitic stainless steels samples in NaH_2PO_4 0.1 mol/L, pH 6.0., at room temperature ($25 \pm 1^\circ\text{C}$).

VoltaMaster 4 program was used to extract zero current potential (ZCP) and corrosion current density (i_{corr}) values from the cyclic potentiodynamic polarization plot. The ZCP was increased from -481 mV for the untreated sample to 332 mV for the nitrided sample. The ZCP obtained from polarization curves for the austenitic stainless steels samples maintained for 2 hours in NaH_2PO_4 0.1 mol/L, pH 6.0 are in agreement with the open circuit potential data. The corrosion current density decrease from $2.5 \mu\text{A}/\text{cm}^2$, registered for untreated sample, to $0.8 \mu\text{A}/\text{cm}^2$, for the nitrided sample.

The current exhibited negative hysteresis when the scan was reversed and pits were not found on the samples after the polarization test. Examination by scanning electron microscopy (SEM) of the surface after anodic polarization indicates a uniform attack (pits were not found) for both austenitic stainless steels (untreated and nitrided) samples tested (Fig. 4).

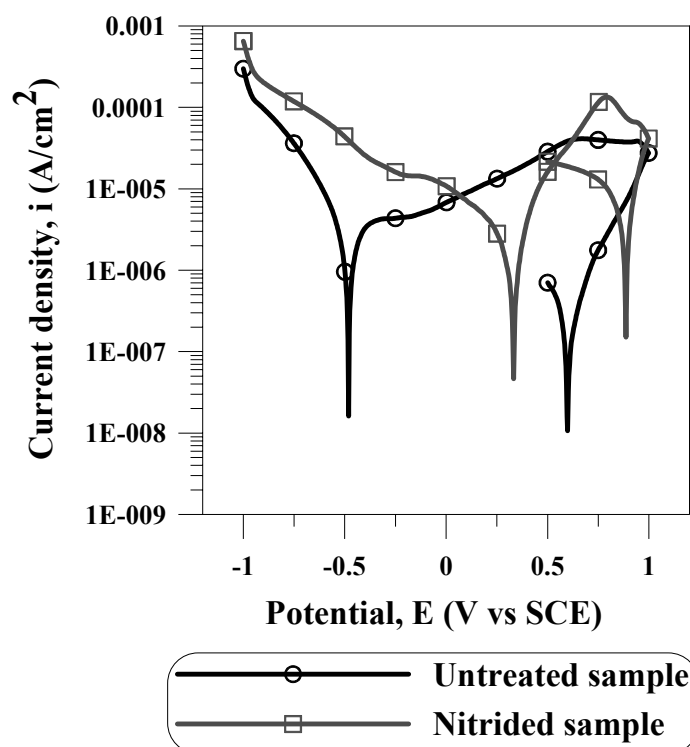


Fig. 3 – Cyclic polarization curves for both untreated and nitrided austenitic stainless steels samples maintained 2 hours in NaH_2PO_4 0.1 mol/L, pH 6.0.

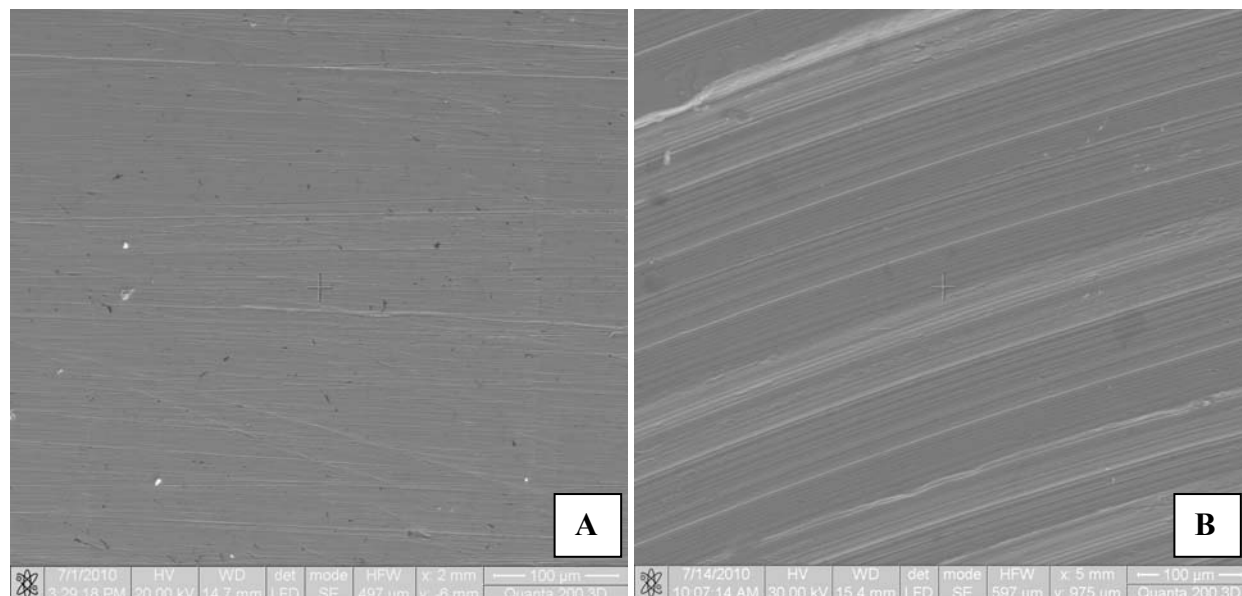


Fig. 4 – Surface attack morphology: (A) untreated sample, (B) nitrated sample.

In a complementary study, electrochemical impedance spectroscopy (EIS) was used to investigate the corrosion resistance of the untreated and nitrated austenitic stainless steels samples in NaH_2PO_4 0.1 mol/L, pH 6.0. The advantage of using this technique lies in the fact that it provides information on the corrosion resistance of the electrodes, and the nature of the electrode/solution interface, under nearly non-polarizing conditions. The experimental impedance data obtained, at E_{OC} with the untreated and nitrated austenitic stainless steels samples immersed for different periods of time are presented as Bode plots in Figs. 5-6. From the Bode spectra it is possible to indicate the presence of a compact passive film if: (a) the phase angle is close to -90° over a wide frequency range and (b) if the spectrum shows linear portions at intermediate frequency. The impedance (Z) of untreated austenitic stainless steels sample increases with the time of electrode immersion. All the spectra show that in a higher frequency region, $\log Z_{mod}$ tends to become constant. This is a typical response for the resistive behaviour and corresponds to the solution resistance, R_{sol} . In the medium frequency range, a linear relationship between $\log Z_{mod}$ and \log Frequency is observed, but with different slopes (always less than -1) and phase angle maxim (less than -90°), indicating that the passive films were not fully capacitive. The impedance spectra found for untreated austenitic stainless steels sample exhibited a near capacitive response illustrated by a phase angle close to -80° in medium frequency range. A near capacitive behaviour, typical for passive materials, is indicated by medium to low frequency by phase angle

approaching -80° , suggesting that a stable film is formed on the tested alloy in the electrolyte used.

High impedance values (order of $10^5 \Omega \text{ cm}^2$) were obtained from medium to low frequencies for untreated austenitic stainless steel suggesting high corrosion resistance in the corrosion medium used.

One peak observed in phase angle plots indicates the involvement of single-time constant at E_{OC} , for untreated austenitic stainless steels samples immersed in NaH_2PO_4 0.1 mol/L, pH 6.0. This behaviour usually indicated that a thin passive oxide layer was formed on the surface.²⁰ The phase angle maxim increases in time.

For the interpretation of the electrochemical behaviour of a system from EIS spectra, an appropriate physical model of the electrochemical reactions occurring on the electrodes is necessary. The electrochemical system may be represented by an equivalent circuit (EC). The impedance spectra were fitted using the ZSimpWin software. Simple equivalent circuit (EC) comprised of only one time constant (Fig. 7a) was used to model the experimental spectra, and good agreement between experimental data and fitted data was obtained. The fitting quality of EIS data was estimated by both the chi-square (χ^2) test (between 10^{-4} and 10^{-5}) values and the comparison between error distribution versus frequency values ($\pm 3\%$ for the whole frequency range) corresponding to experimental and simulated data. The R_1 and Q_1 parameters describe the processes occurring at electrolyte/passive film interface. R_{sol} is the ohmic resistance of the electrolyte. The same R_{sol} value, that is $173 \pm 3 \Omega$, was noticed in all the cases.

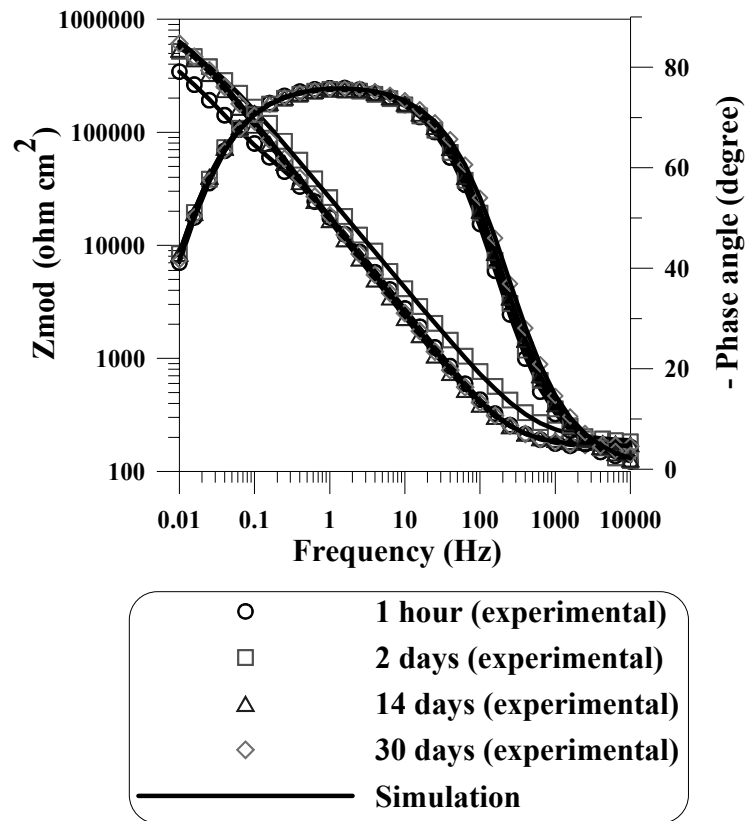


Fig. 5 – Representative Bode plots for untreated sample maintained different time in NaH_2PO_4 0.1 mol/L, pH 6.0, at E_{OC} .

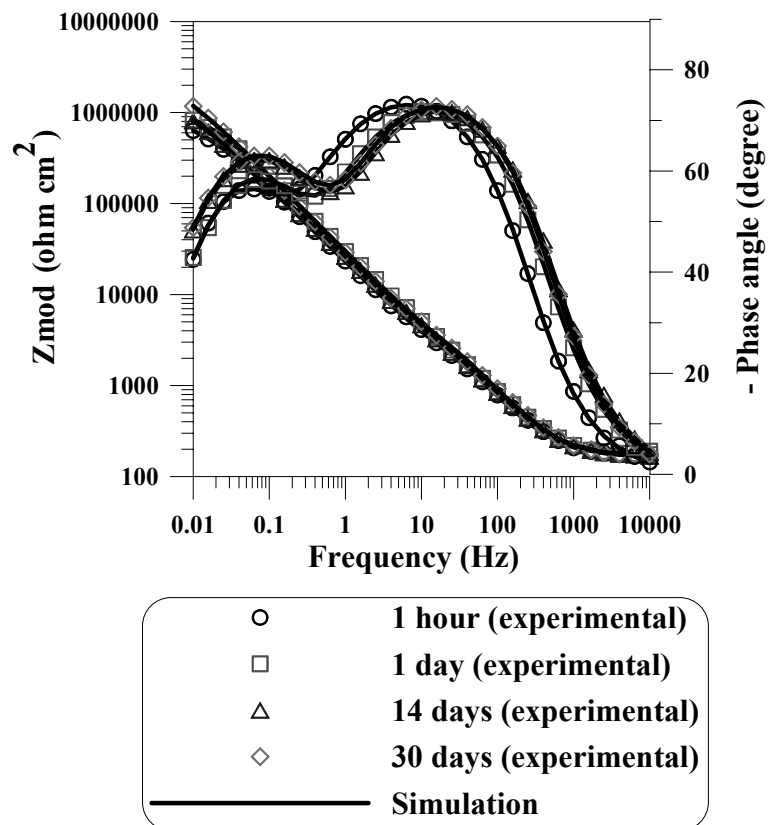


Fig. 6 – Representative Bode plots of plasma nitrided austenitic stainless steel maintained different time periods in NaH_2PO_4 0.1 mol/L, pH 6.0, at E_{OC} .

The symbol Q signifies the possibility of a non-ideal capacitance (CPE, constant phase element). The CPE considers the fact that, experimentally, the barrier film never exhibits the theoretically expected phase shift of -90° and a slope of -1 for an ideal dielectric. The impedance of the CPE is given by:²¹

$$Q = Z_{CPE} = \frac{1}{C(j\omega)^n} \quad (1)$$

where for $n = 1$, the Q element reduces to a capacitor with a capacitance C and, for $n = 0$, to a simple resistor. n is related to a slope of the $\log Z_{mod}$ vs. \log Frequency Bode-plots, ω is the angular frequency and j is imaginary number ($j^2 = -1$).

Large value of R_1 , at E_{OC} was obtained supporting the passivation of untreated austenitic stainless steel sample immersed in NaH_2PO_4 0.1 mol/L, pH 6.0. The resistance element, R_1 increases with increasing immersion time (from $3.6 \times 10^5 \Omega \text{ cm}^2$ after 1 hour immersion time to $6.5 \times 10^5 \Omega \text{ cm}^2$ after 30 days immersion time). The n_1 values corresponding for untreated austenitic stainless steels samples varying from 0.82 to 0.86 indicate the deviation from near capacitance behaviour. The low constant phase elements, Q_1 , (from $1.6 \times 10^5 \text{ S cm}^{-2} \text{ s}^n$ after 1 hour immersion time to $1.1 \times 10^5 \text{ S cm}^{-2} \text{ s}^n$ after 30 days immersion time), support the other results of this study, which indicate the passive behaviour of the untreated austenitic stainless steel. Although the actual value of the dielectric constant within the passive film is difficult to estimate, a change of Q_1 can be used as indicator for the changes in the passive film

thickness. Assuming the dielectric constant does not change with the different parameters under investigation; the reciprocal capacitance of the passive film ($1/Q_1$) is directly proportional to the thickness of the passive film. The resistance, R_1 , and the thickness, $1/Q_1$, of the passive film increase with the immersion time indicating a continuous growth of the passive film in time until a steady state is attained.

In the case of nitrated austenitic stainless steels samples immersed in NaH_2PO_4 0.1 mol/L, pH 6.0 two relaxation time constants are indicated on phase angle plots. These observed behaviours evinced the presence of a duplex layer over nitrated austenitic stainless steels sample.

The occurrence of a second overlapping wave in the phase shift response signifies that the spectra can no longer be explained by a simple equivalent circuit based on parallel resistance and constant phase element. Fitting of the impedance was done with an EC (Fig. 7b) using a series combination of the solution resistance, R_{sol} (around 173Ω), with two RQ parallel combinations: $R_{sol}(R_1Q_1)(R_2Q_2)$. A very good agreement between the simulated and experimental data was obtained. The experimental data are shown by the symbols and the simulated data (generated using the equivalent circuit), are shown as the solid lines (Fig. 7b). The high-frequency parameters R_1 and Q_1 represent the properties of the reactions at the outer passive film/solution interface. The parameter R_2 coupled with Q_2 describes the processes at the nitrated layer at the electrolyte/nitrated layer interface.

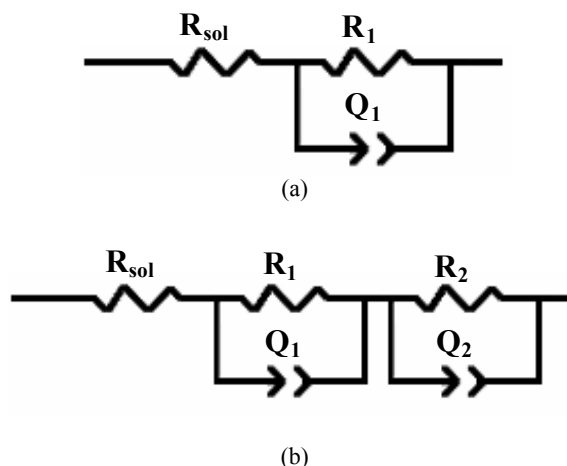


Fig. 7 – Equivalent circuits (EC) used to fit the impedance data.

High resistance values of outer passive layer, R_1 , (around $5 \times 10^4 \Omega \text{ cm}^2$) were found for nitrided sample. These values indicate the formation of a passive layer with good corrosion resistance. The exponent of Q_1 , varied 0.88 to 0.91, which is indicative of near-capacitive behaviour, which coupled with the higher R_1 resistance, tends to suggest a compact outer layer. The n_2 values were approximately 0.84 in the case of Q_2 . This shows that Q_2 contains some frequency dispersion. As immersion time increases from 1 hour to 30 days, nitrided layer resistance (R_2) increase from $6.2 \times 10^5 \Omega \text{ cm}^2$ to $9.8 \times 10^5 \Omega \text{ cm}^2$. For nitrided sample, the R_2 (nitrided layer) is about 10 times higher than the R_1 (passive layer). This reveals that the nitrided layer provides most of the protection.

Polarization resistance (R_p) is represented by the sum of the resistance of the passive layer (R_1) and nitrided layer (R_2). A high R_p value corresponds to a high resistance to passive dissolution. For highly corrosion resistance materials the polariza-

tion resistance (R_p) may even reach $1 \times 10^6 \Omega \text{ cm}^2$.²² This indicates that the nitrided austenitic stainless steels sample immersed in NaH_2PO_4 0.1 mol/L, pH 6.0 are still highly resistant to corrosion.

Fig. 8 schematically shows the possible structures, from a corrosion protection point of view, for the untreated and plasma nitrided austenitic stainless steels samples. The corrosion resistance for the untreated austenitic stainless steel sample was provided only by a passive film (oxide layer) on the surface. The passive film on these austenitic stainless steels surface can protect the material in a low to moderate corrosive environment (NaH_2PO_4 0.1 mol/L, pH 6.0). In comparison, the nitrided austenitic stainless steels sample could still have a thin passive film on the surface and beneath a nitrided layer. Both the passive film and the nitrided layer could have protected the substrate from corrosion.

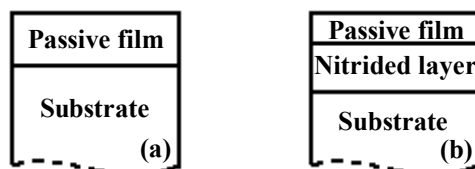


Fig. 8 – Schematic diagrams showing the possible structures in the: untreated (a) and plasma nitrided (b) austenitic stainless steel surfaces.

EXPERIMENTAL

Materials

Samples of austenitic stainless steel (wt. %: 0.02C 18.62Cr 8.04Ni 73.31Fe) were used. Sample about 10 mm thick was cut from incoming bar of 30 mm diameter, and wet ground with SiC paper from 400 down to 2500 grit to produce a fine surface finishing. The austenitic stainless steel sample was plasma nitrided at the Grupo T.T.N. S.P.A. Nitrurazioni Cementazioni Bonifiche Ricotture Tempra Sottovuoto Sale Induzione (Nerviano, Italy) in a DC glow discharge plasma nitriding unit for 14 hours at a temperature of 530°C. The treatment gas was 20% N_2 + 80% H_2 (at. %).

The cross-sectional microstructure of the nitrided samples was observed using an AxioImager A1m type optical microscopy (OM).

The tests specimens were in a polytetrafluoroethylene holder specifically designed to connect to a rotating disc electrode (type EDI 101T; Radiometer Analytical, Villeurbanne, France). Prior to corrosion electrochemically tests, the untreated samples were wet-ground with 400, 600, 1000, 1500 and 2000 grit metallographic abrasive papers, final polishing was done with 1 μm alumina suspension.

The solution was prepared using double-distilled water and sodium dehydrogeno-phosphate p.a. in a concentration of 0.1 mol/L and pH adjusted to 6.0 with sodium hydroxide

solution. Corrosion tests were performed at room temperature ($25 \pm 1^\circ\text{C}$).

The electrochemical measurements were made with a potentiostatic assembly of three electrodes: a working electrode (rotating electrode), a platinum counter-electrode and a reference electrode of saturated calomel (SCE). All potentials referred to in this article are with respect to SCE. Given the diffusion phenomena that play a major role with regard to the changes which are produced on the metal/solution interface and consequently on the state and composition of the layers of the metal surfaces, readings were taken in a laminar system (criterion $Re < 2300$) with a rotational velocity at 500 rpm in order to control the mass transfer phenomena. The measurement system was managed by a VoltaLab 40 potentiostat controlled by a personal computer with dedicate software (VoltaMaster 4).

For both samples (untreated or nitrided), 2 hours open circuit potential (E_{OC}) measurement was performed initially followed by the cyclic potentiodynamic polarization measurement. These tests were conducted by stepping the potential using a scanning rate of 1 mV/s from -1000 mV (SCE) to +1200 mV (SCE) and reverse to +500 mV (SCE). Using an automatic data acquisition system, the potentiodynamic polarization curves were plotted and both corrosion current density (i_{corr}) and zero current potential (ZCP) were estimated by Tafel plots by using both anodic and cathodic branches.

Electrochemical impedance spectroscopy (EIS) was also used to evaluate the samples. The alternating current (AC) impedance spectra for both samples were obtained, with a scan frequency range of 10 kHz to 10 mHz with amplitude of 10 mV. EIS measurements were performed in aerated solution. The EIS data were registered at open circuit potential for both samples at different immersion time in solution, at 25°C. In order to supply quantitative support for discussions of these experimental EIS results, an appropriate model (Convertor-Radiometer, France and ZSimpWin-PAR, USA) for equivalent circuit (EC) quantification has also been used.

CONCLUSIONS

Very low corrosion current densities were obtained for both untreated and nitrided austenitic stainless steel samples tested in NaH₂PO₄ 0.1 mol/L, pH 6.0. Over the surface of the untreated and nitrided austenitic stainless steel samples a uniform corrosion appears. The EIS results show that untreated and nitrided austenitic stainless steel samples exhibit passivity at open circuit potential. For both samples (untreated and nitrided) the polarization resistance is increasing with the immersion time because of the surface passivation. The EIS results of the nitrided austenitic stainless steel samples in NaH₂PO₄ 0.1 mol/L, pH 6.0 can be fitted using the model of R_{sol}(R₁Q₁)(R₂Q₂) and of the untreated austenitic stainless steel samples in the same solution can be fitted using the model of R_{sol}(R₁Q₁). These results confirm the presence of a two layer film consisting of an inner nitrided layer responsible for the corrosion protection, and of an outer passive film on the surface of the nitrided austenitic stainless steel samples in NaH₂PO₄ 0.1 mol/L, pH 6.0 and a single passive film on the surface of the untreated austenitic stainless steel samples in the same solution. In NaH₂PO₄ 0.1 mol/L, pH 6.0, the nitrided austenitic stainless steel sample surfaces have a corrosion behaviour better or similar to the untreated austenitic stainless steel.

REFERENCES

1. J. Flis, J. Mankouski and E. Rolinski, *Surf. Eng.*, **1989**, *5*, 151-157.
2. E. Rolinski, *Surf. Eng.*, **1987**, *3*, 35-40.
3. T. Bell and K. Akamatsu, "Stainless Steel 2000 – Thermochemical Surface Engineering of Stainless Steel", The Institute of Materials, 2001.
4. M. Samandi, B.A. Sheddou, D.I. Smith, G.A. Collins, R. Hutchings and J. Tendys, *Surf. Coat. Technol.*, **1993**, *59*, 261-266.
5. G.S. Chang, J.H. Son, S.H. Kim, K.H. Chae, C.N. Whang, E. Menthe, K.-T. Rie and Y.P. Lee, *Surf. Coat. Technol.*, **1999**, *112*, 291-294.
6. E. Menthe and K.-T. Rie, *Surf. Coat. Technol.*, **1999**, *116*, 199-204.
7. S. Parascandola, W. Möller and D. Williamson, *Appl. Phys. Lett.*, **2000**, *76*, 2194-2196.
8. X.Y. Li, *Surf. Eng.*, **2001**, *17*, 147-153.
9. S. Picard, J.B. Memet, R. Sabot, J.L. Grosseau-Poussard, J.-P. Rivière and R. Meilland, *Mater. Sci. Eng. A*, **2001**, *303*, 163-172.
10. J. Feugeas, B. Gomez and A. Craievich, *Surf. Coat. Technol.*, **2002**, *154*, 167-175.
11. L.L. Pranevicius, P. Valatkevicius, V. Valincius, C. Templier, J.-P. Rivière and L. Pranevicius, *Surf. Coat. Technol.*, **2002**, *156*, 219-224.
12. L.C. Gontijo, R. Machado, S.E. Kuri, L.C. Casteletti and P.A.P. Nascente, *Thin Solid Films*, **2006**, *515*, 1093-1096.
13. C.X. Li, T. Bell, *Corrosion Sci.*, **2006**, *48*, 2036-2049.
14. Al. Banu, M. Marcu, O. Radovici, C. Pirvu and M. Vasilescu, *Rev. Roum. Chim.*, **2006**, *51*, 193-198.
15. V. Brânzoi, F. Brânzoi, A. Stanca and L. Mititeanu, *Rev. Roum. Chim.*, **2008**, *53*, 459-469.
16. Al. Banu, M. Marcu and O. Radovici, *Rev. Roum. Chim.*, **2008**, *53*, 941-945.
17. J.F. McCabe, "Applied dental materials", 7th edition, Blackwell Science Publication, Oxford, 1994.
18. T.M. Muraleedharan and E.I. Meletis, *Thin Solid Films*, **1992**, *221*, 104-113.
19. V. Singh and E.I. Meletis, *Surf. Coat. Technol.*, **2006**, *201*, 1093-1101.
20. E. Kobayashi, T.J. Wang, H. Doi, T. Yoneyama and H. Hamanaka, *J. Mater. Sci. Mater. Med.*, **1998**, *9*, 567-574.
21. I.D. Raistrick, J.R. Macdonald and D.R. Francschetti, "Impedance Spectroscopy Emphasizing Solid Materials and Systems", John Wiley&Sons, New York, 1987.
22. F. Mansfeld, *J. Electrochem. Soc.*, **1973**, *120*, 515-518.